An Improved Toner Flow Model for Dual-Component Magnetic Brush Development*

Masayasu Anzai and Yohsuke Saitoh
Katsuta Research Laboratory, Hitachi Koki Co., Ltd.
1,060 Takeda, Hitachinaka City, Japan

Abstract

The deposition of toner on a latent electrostatic image is a function of the toner flow rate in the development region of a dual-component magnetic brush development system. Some models have been previously proposed to describe the dependence of development on the speed ratio between the magnetic brush and the recording medium. We propose an improved toner flow model that considers the speed difference between the developer brush and the electrostatic image. This model presents the toner flow mass as a function of the product of the brush speed ratio and a saturation function of the brush speed difference. The model is useful for predicting the deposited toner mass and optical image density when the development conditions are changed. Analytical and experimental studies are described. The experimental results correspond well with the calculated results.

Introduction

Magnetic brush development with a dual-component developer consisting of toner and magnetic carrier beads is the most common method of development of electrostatic latent image in electrophotography or electrostatic recording. The surface of an electrostatic latent image is brushed by the tip of the magnetic brush of the developer formed on a magnetic roller. Although the development process and the behavior of developing toner are complicated, they are important, because they influence the development characteristics and the image quality. In this development process, toner flows to the development region, where it deposits on the surface of the electrostatic latent image. The toner mass deposited on the surface of the recording medium is determined by the toner flow rate into the developing region (where the brush nip touches the surface) and the toner deposition rate.

In analysis and experiments concerning this process, many studies have been carried out and a number of models have been proposed during the past 20 years or more. The literature topics include toner deposition analysis,[1–8] microscopic analysis[2,6,9] macroscopic analysis,[10] field stripping theory,[1,5,6] powder cloud theory,[11,12] equilibrium theory,[3] space-charge effect,[10] depletion phenomenon,[13] dip phenomenon,[3,6] ordinary differential equation approach,[9] geometric flow model,[14] toner supply rate limit model,[15] and electrical properties of brush development.[16,17] In these studies, the toner flow mass depends on the speed ratio between the magnetic brush and the recording medium. The deposited toner mass depends on the electrostatic field of the latent image, the magnitude of the toner charge, and the scavenging force. The system is complicated, and it is difficult to obtain an exact quantitative solution because the development process has many parameters. The dip phenomenon occurring at the point of brush speed synchronized with that of the recording medium is treated as a special case, although it is noted that the cause is either the decrease of shear force[3] or toner depletion.[13,14]

This study proposes an improved toner flow model[18] based on both the speed ratio of the magnetic brush and the recording medium and the perturbation of developer materials caused by the speed difference. This model is simple, but useful, for examining the dynamic characteristics of development machines, including the dip phenomenon.

Proposed Toner Flow Model

Figure 1 shows development schemes for a dual-component magnetic brush development. Toner particles are transported by carrier beads into the development region. The developer brush contacts the surface of a recording medium having an electrostatic latent image with the brush nip width W, as shown in Figure 1(a). Toner particles deposit on the surface through a balance of electrostatic and kinetic forces, as shown in Figure 1(c).[3] The shape of the brush, the collision force of the rising carrier bead chains of the brush, and the shear force due to the speed difference make the beads move or rotate, as shown in Figure 1(b). This perturbation or agitation causes the toner flow mass to increase. Therefore, the toner flow mass in solid area development is determined by the product of the brush speed ratio and the perturbation of the developer. In the case of line images, as shown in Figure 1(a), it is necessary to consider the depletion effects[14] of line width L_2, line pitch L_1, and brush nip width W. The perturbation of the developer occurs independently of the electrical resistance of the developer. Therefore, this flow model is appropriate for both insulative developers and conductive developers.

As the developer perturbation is increased by an increase in the speed difference between the brush and the latent image, it is thought that the differential of perturbation with respect to brush speed difference is proportional to the perturbation difference from the saturation value.

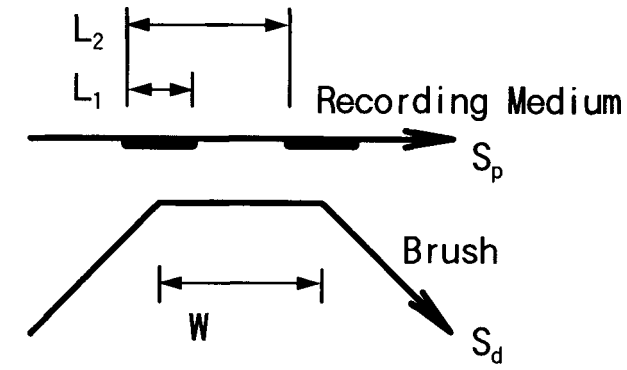

(a)

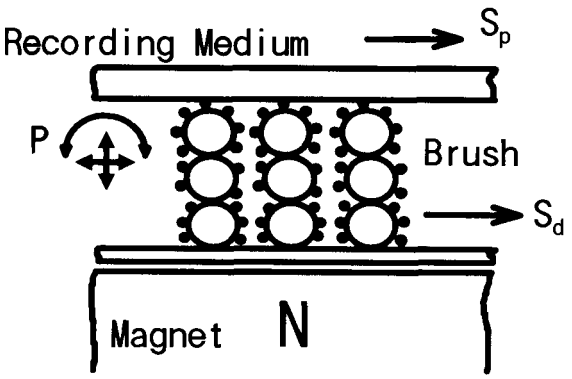

(b)

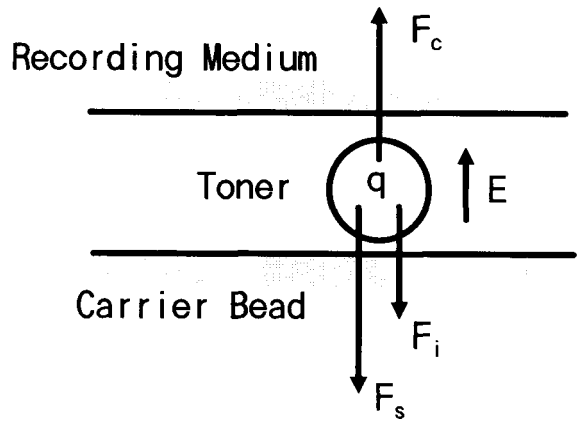

(c)

Figure 1. Development schemes for a dual-component magnetic development system. (a) shows the developer conveyance (S_p, recording medium speed; S_d brush speed; L_1, line pitch; L_2, line width; W, brush nip width), (b) shows the movement of carrier bead chains (P, perturbation of the developer); (c) represents toner deposition (q, toner charge; F_c Coulombic force qE; F_i, image force $\propto 1/q^2$; F_s, scavenging force; E, electrostatic field strength).

Thus

$$P_0 - P = \eta \cdot dP / dJ, \tag{1}$$

where

P_0	= saturation value of perturbation
$P(= p \cdot W)$	= magnitude of perturbation
p	= perturbation per unit brush nip width
W	= brush nip width
η	= coefficient
$J = \lvert S_d - S_p \rvert$	= brush speed difference
S_d	= brush speed
S_p	= recording medium speed,

and where S_d is positive for the with-mode operation. Solving this, the perturbation is given by

$$\begin{aligned} P &= P_1 + (P_0 - P_1)\{1 - \exp(-J / \eta)\}, \\ &= P_1 \cdot [1 + \lambda \cdot \{1 - \exp(-J / \eta)\}] \end{aligned} \tag{2}$$

for P_1 = perturbation at $J = 0$ and λ = perturbation coefficient. Rewritten as a function of the speed ratio between the brush and the latent surface,

$$P = P_1 \cdot [1 + \lambda \cdot \{1 - \exp(-\lvert S - 1 \rvert / v)\}] \tag{3}$$

for $v = \eta / \lvert S_p \rvert$ and $S = S_d / S_p$, the speed ratio. Eventually the toner flow mass is

$$H = (a + P \cdot u)h, \tag{4}$$

When P is large or "a" can be included in P,

$$H = P \cdot u \cdot h, \tag{5}$$

where

H	= toner flow mass
a	= toner weight per unit area of the brush surface
u	= toner weight per unit volume of the developer
h	= geometric function proposed by Vahtra[14]

and where h gives for $L_1 - L_2 \leqq W \cdot \lvert 1 - 1/S \rvert$

$$h = L_1 / L_2 \cdot \lvert S \rvert \tag{6}$$

with L_1 as line pitch and L_2 as line width. Then, for $L_1 - L_2 \geqq W \cdot \lvert 1 - 1/S \rvert$, h gives

$$h = (S_d - S_p)/\lvert S_d - S_p \rvert \cdot W/L_2 \cdot (S - 1) + \lvert S \rvert \tag{7}$$

for solid images, $L_1 = L_2$ in Eq. 6 or $L_2 = \infty$ in Eq. 7:

$$h = \lvert S \rvert. \tag{8}$$

When multiple development rollers are employed, the toner flow mass can be treated as the sum of the values for each roller:

$$\begin{aligned} H_s &= \Sigma H_n = \Sigma\,(P \cdot u \cdot h)_n \\ &= \Sigma(u \cdot h \cdot P_1 \cdot [1 + \lambda \cdot \{\gamma - \exp\,(-\lvert S - 1 \rvert / v)\}])_n, \end{aligned} \tag{9}$$

where

H_s	= total flow mass
H_n	= flow mass of nth development roller
n	= number of development rollers.

A schematic curve of the toner flow mass H for solid images is illustrated in Figure 2. The dip at $S = 1$ can be described.

From the above considerations, the next step will be clear. To increase H for solid images, not only the speed ratio, S, but also P_1, λ, η, J, and u are effective. A developer

having small-diameter carrier beads gives a large H value because of the large u: that is, high toner mass per unit volume of the developer for the same toner coverage ratio on the carrier bead surface. When process speed, S, becomes low, the same deposit toner mass M cannot be obtained if the same S is used.

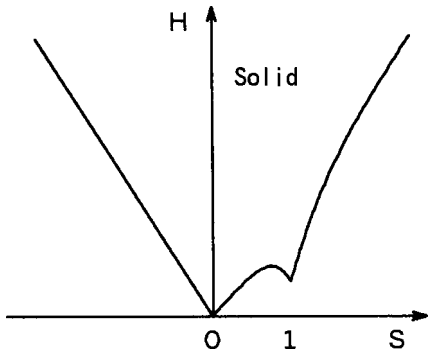

Figure 2. Schematic illustration of toner flow mass.

Toner deposition progresses through a balance of electrostatic force and kinetic force. Therefore, the differential of the deposited toner mass with respect to toner flow mass is proportional to the toner-depositing potential. Thus,

$$M_0 - M = \psi \cdot dM/dH, \tag{10}$$

where M_0 = saturation value of deposit toner mass
M = deposit toner mass
ψ = coefficient.

This gives

$$M = M_0 \cdot \{1 - \exp(-H/\psi)\}. \tag{11}$$

Considering the scavenging force of the magnetic brush and the image force with toner charge to a carrier bead, as shown in Figure 1(c), M_0 is presented as follow:[19]

$$M_0 = \kappa_1 \cdot E/q - \kappa_2 \cdot F_s/q^2 - \kappa_3 \tag{12}$$
$$= \kappa_1 \cdot \{E - (\kappa_4 \cdot F_s/q + \kappa_5 \cdot q)\}/q$$
$$\equiv \kappa_1 \cdot E_e/q, \tag{13}$$

where E = electrostatic field strength of a latent image
E_e = effective electrostatic field strength of a latent image
F_s = scavenging force
q = toner charge deposited
$\kappa_1, \kappa_2, \kappa_3, \kappa_4, \kappa_5$ = coefficients.

Scavenging force F_s will also be a function of S_d.

Toner mass on the paper after transfer is given as

$$M_p = M - M_r, \tag{14}$$

where M_p = transferred toner mass and M_r = residual toner mass on a recording medium. Transfer effieiency is

$$\tau = 1 - M_r/M, \tag{15}$$

where M_r is generally a function of M, but it is nearly constant when the transfer electrostatic field strength is strong enough.

Then the optical density of the image can be described by an experimental equation:

$$D = D_p + D_t \cdot [1 - \exp\{-(M_p - M_s)/\mu\}], \tag{16}$$

where D = optical density of image
D_p = optical density of paper
D_t = saturation value of optical density of toner images
M_s = toner mass on the threshold of optical density
μ = coefficient.

Comparison of Expressions for Solid Image Mass

The expressions for deposited toner mass of solid images by representative models of former studies and this model are enumerated below as functions of brush speed ratio S. Only the improved model presented here is able to describe the dip at $S = 1$.

1. Equilibrium theory,[2,3] and geometric model[14]:

$$M = k_1 \cdot |S| \tag{17}$$

2. Electrostatic field stripping model[1]:

$$M = k_2 \cdot \{1 - \exp(-k_3 \cdot |S| \cdot t)\}, \tag{18}$$

where t is the developing time.

3. Electrostatic potential analysis[7]:

$$M = k_4 (-A + [A^2 + B\{1 - \exp(-k_5 \cdot |S| \cdot n)\}]^{0.5}) \tag{19}$$

$$\doteq k_6 \{1 - \exp(-k_5 \cdot |S| \cdot n)\}, \tag{20}$$

where n is the number of development times or rollers.

4. Toner flow model presented here: Combining Eq. 11 with Eqs. 8 and 9, we obtain

$$M = k_7 \cdot \{1 - \exp(-k_8 \cdot H_s)\}, \tag{21}$$

where $H_s = \sum[k_9 \cdot |S| \cdot (1 + k_{10}\{1 - \exp(-k_{11} \cdot |S - 1|)\})]_n$.

Table I. Experimental Conditions and Materials

Process speed	S_p: 119 or 254 mm/s
Latent image	Surface voltage V_0: 750 V
	Residual voltage V_r: 50 or 75 V
Development	Brush speed ratio S: –3~3
	Development roller diameter Φ_d: 40 or 57mm
	Doctor/development gap G_{doc}/G_{dev}: 0.6/1.0, 0.8/1.0 or 1.3/1.6 mm
	Development bias voltage V_b: 300, 400, or 500 V
Developer A	Carrier: ferrite ϕ90 μm, 10^8 cm
	Toner: ϕ10.3 μm, 19 μC/g
	Toner concentration: T_c = 4 wt%
Developer B	Carrier: ferrite ϕ120 μm, 10^6 cm
	Toner: ϕ10.8 μm, 17 μC/g
	Toner concentration: T_c = 4 wt%

Experiments and Discussion

A laser printer was used for our experiments. A dielectric belt toner transfer system, an electrostatic field toner cleaner, and a heat pressure roll toner fuser were utilized. The photoreceptor is a double-layer type 17 μm in thickness, and the drum diameter is 120 mm. The strength of the development magnet was about 0.1 T (1000 G). Other experimental conditions and materials are listed in Table I. Using this apparatus, the optical image density and the developed toner mass on the photoreceptor were investigated by reversal development. Each condition was selected according to an experimental objective and convenience.

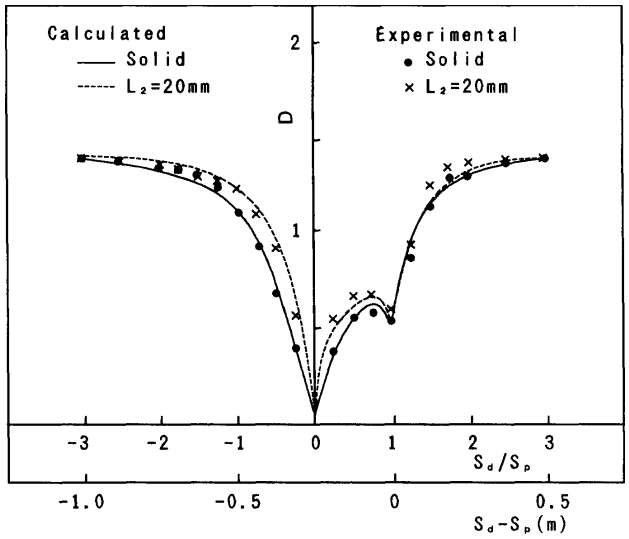

Figure 3. Relationship between brush speed and image density. Experimental conditions (Developer A: S_p, 254 mm/s; V_b, 400 V; V_r, 50 V; G_{doc}/G_{dev}, 0.8/1 mm; Φ_d, 57 mm), calculated conditions ($P_1 \cdot u/\psi$, 0.22; λ, 2.1; ν, 0.71; M_0, 1 mg/cm^2; D_p, 0.08; D_t, 1.46; M_s, 0; M_r, 0.06 mg/cm^2; μ, 0.35; W, 4 mm; L_1, 60 mm; L_2, 20 mm).

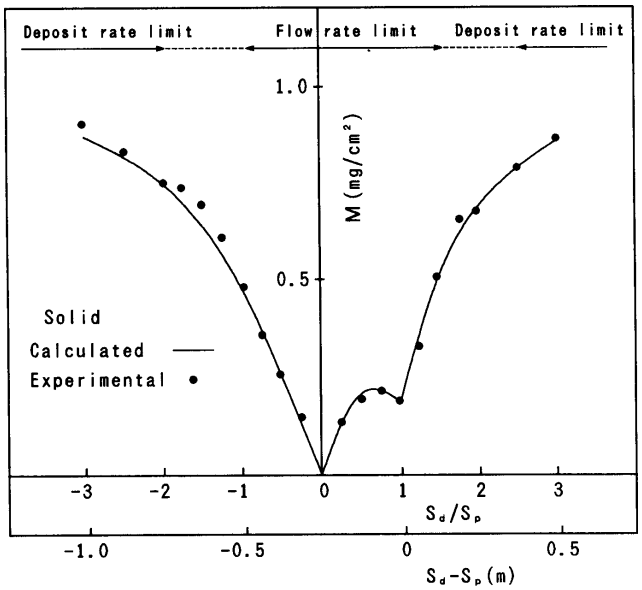

Figure 4. Relationship between brush speed and developed toner mass for solid images. Experimental and calculated conditions are as in Fig. 3.

The influences of brush speed ratio on optical image density and deposit toner mass are shown in Figures 3 and 4, respectively. Solid lines and broken lines show calculated values. The parameters used for the calculations were determined by fitting the calculated values to the experimental values. In the calculation, we assume that brush nip width W is half the value calculated as brush thickness, which is the doctor gap plus 0.6 mm, because of packing density of the magnetic brush.

The calculation corresponds well with the experiment. The dip phenomenon was observed in both the solid image and the line image at $S = 1$. Note that toner deposit mass M increases in linear proportions to the increase in brush speed ratio S from 0 to –1 where M is less than about 0.5 mg/cm^2 in the "against" mode of development in Figure 4. Then M begins to saturate. Therefore, a flow-rate limit region is that in which S equals from –1 to 1.5, and deposit-rate limit regions are those in which S is less than –2 or greater than 2.5. The increase of M by brush speed difference J began to saturate at about 30 cm/s. These results show that the developer perturbation contributes to the increase of toner flow mass in the development process.

The influence of development bias voltages on image density as a function of brush speed ratio is given in Figure 5. Each point represents an experimental value, and solid lines represent calculated values. In the calculation, M_0 was varied according to development bias voltage, assuming that M_0 was in linear proportion to the development latent voltage. Good correspondence between the experiment and calculation was obtained. From the fact of the dependence on the development bias voltage in the flow-rate limit region where S is between –1 and 1.5 as mentioned regarding Figure 4, it is known that complete depletion does not yet occur and a part of toner flow mass is able to deposit.

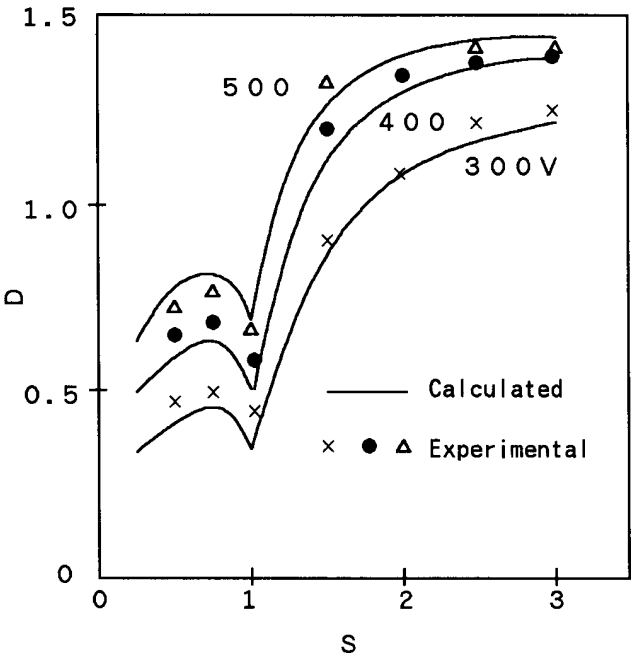

Figure 5. Influence of development bias voltages. Experimental and calculated conditions (V_r, 75 V; M_0, 0.64, 0.93, and 1.22 mg/cm^2 for V_b = 300, 400, and 500 V; other conditions are as in Fig. 3).

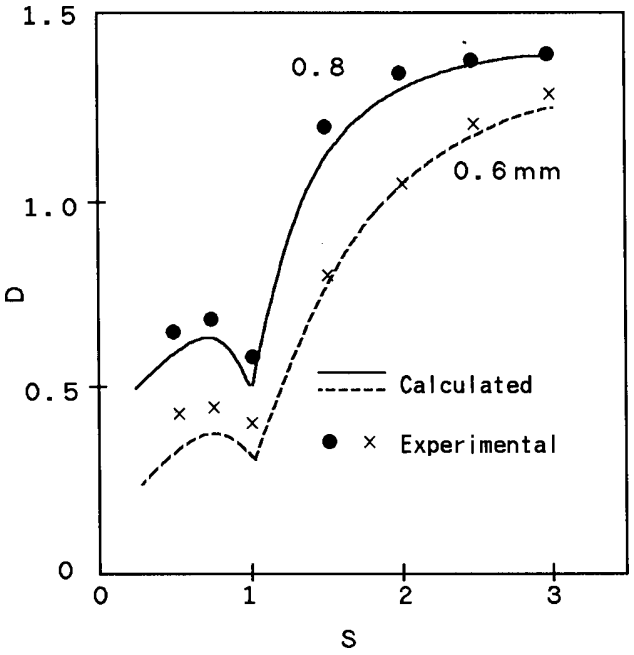

Figure 6. Influence of doctor gaps. Experimental and calculated conditions (V_r, 75 V; G_{dev}, 1 mm; $P_1 \cdot u/\psi$, 0.15 and 0.22 for G_{doc} = 0.6 and 0.8 mm; λ, 1.6 and 2.1 for G_{doc} = 0.6 and 0.8 mm; W, 2.8 and 4 mm for G_{doc} = 0.6 and 0.8 mm; M_0, 0.93 mg/cm^2; other conditions are as in Fig. 3).

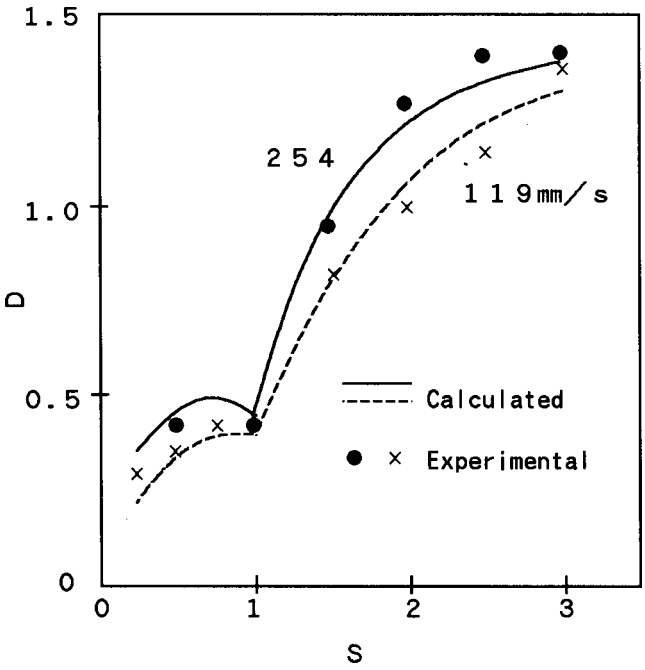

Figure 7. Influence of process speeds. Experimental conditions (Developer B: V_b, 400 V; V_r, 50 V; G_{doc}/G_{dev}, 1.3/1.6 mm; Φ_d, 40 and 57 mm for S_p = 119 and 254 mm/s); calculated conditions ($P_1 \cdot u/\psi$, 0.15 and 0.17 for S_p = 119 and 254 mm/s; λ, 1.8; v, 1.78 and 0.83 for S_p = 119 and 254 mm/s; M_0, 1 mg/cm^2; W, 3.1 and 3.5 mm for S_p = 119 and 254 mm/s; other conditions are as in Fig. 3).

When the packing density of a developer in the brush nip region changes, the perturbation will change. Low packing density will give small perturbation. To investigate its influence, the packing density was varied by using selected doctor gaps. The result is shown in Figure 6. In the calculation, the values of P_1, u, and λ were based on an assumed linear approximation. The calculated values correspond roughly with the experimental values.

The influence on photoreceptor speed S_p is shown in Figure 7. According to this model, when S_p becomes low, the toner deposit mass can't be obtained if the brush speed ratio S is kept constant. Experimental and calculated results proved it. In this experiment a second developer, Developer B was used, so that the fundamental parameters for the calculation were changed. The effect of the different development roller diameter was also compensated for in the calculation.

Through the analytical and experimental investigation concerning this model, it is clear that the perturbation is related to the increase of toner flow mass. To learn the cause of the perturbation, brushing force was measured in another experiment, using a similar development apparatus. It was confirmed that the greatly increased ratio of brushing force appeared at speed differences less than about 0.5 m/s. From this observation, it is known that brushing force or shear force may contribute to the perturbation.

To increase toner flow mass or to suppress the dip, the release of the carrier beads from the chains of the brush and the imposition of electromagnetic or mechanical vibration on the tip of the brush may be effected by (1) use of a special development magnet, for example, a wide-pole magnet or a double-pole magnet, (2) rotation of both a magnetic roller and a sleeve roller, (3) supply of ac voltage as additional biasing, and/or (4) use of carrier beads having low saturated magnetization.

Conclusions

In support of the proposed toner flow model in a dual-component magnetic brush development system, the following results were obtained:

1. The model considered that the effect of the brush speed difference on developer perturbation can describe well the development properties.
2. The toner flow mass is considered to be a function of the product of the brush speed ratio and a saturation function of the brush speed difference.
3. The deposited toner mass is dominated by the toner flow limit or by the toner deposit limit, according to the toner flow mass as the brush speed is changed.

Acknowledgment

The authors would like to thank Mr. S. Nishino, Mr. Y. Fujinuma, and Mr. J. Kobayashi for their help in the experiments.

References

1. G. Harpavat, *IEEE-IAS Annual Conf. Proc*., 128 (1975).
2. L. B. Schein, *IEEE-IAS Annual Conf. Proc*., 140 (1975).
3. L. B. Schein, *Photogr. Sci. Eng.* **19** (5): 255 (1975).
4. N. Kutuvada and Y. Ando, *Oyo-Buturi (Appl. Phys.)* **39** (5): 406 (1975).
5. A. Kondo and M. Kamiya, *TAPPI* **59** (10): 94 (1976).
6. E. M. Williams, *IEEE-IAS Annual Conf. Proc.,* 215 (1978).
7. J. Nakajima, M. Kimura, M. Horie, and H. Takahashi, *Denshi-Shashin-Gakkai-shi (Electrophotography)* **19** (2): 10 (1981).
8. T. Teshigawara, H. Tachibana, and K. Terao, *IEEE-IAS Annual Conf. Proc.* 1520 (1985).
9. J. A. Benda and W. J. Wnek, *IEEE Trans. Industry Appl.* **IA-17** (6): 610 (1981).
10. E. M. Williams, *The Physics and Technology of the Xerographic Process*, John Wiley, New York, 1984, p.165.
11. W. Verlinden, J. V. England, and J. V. Biessen, *Paper Summaries*, *SPSE's 3rd International Conference on Electrophotography,* 1977, p. 49 .
12. J. V. England, *Photogr. Sci. Eng.* **23**, 86 (1979).
13. L. B. Schein, *Electrophotography and Development*, 2nd ed., Springer-Verlag, Berlin, 1992, p. 152.
14. U. Vahtra, *Photogr. Sci. Eng*. **26**: 292 (1982).
15. J. J. Folkins, *Proceedings of SPSE's 6th International Congress on Advances in Non-Impact Printing Technologies,* 1990, p. 15.
16. Dan A.Hays, *J. Imaging Technol*. **15**: 29 (1989).
17. T. Kurita, *Proceedings of IS&T's 7th International Congress on Advances in Non-Impact Printing Technologies*, 1991, p. 147.
18. M. Anzai and Y. Saitoh, *Proceedings of IS&T's 11th International Congress on Advances in Non-Impact Printing Tech nologies*, 1995, p. 256.
19. M. Anzai, N. Hoshi, H. Sawada, and A. Shimada, *Denshi-Shashin (Electrophotography)* **24**: 11 (1985).